Journal of Experimental Botany, Vol. 62, No. 13, pp. 4521–4531, 2011
doi:10.1093/jxb/err160 Advance Access publication 9 June, 2011
This paper is available online free of all access charges (see http://jxb.oxfordjournals.org/open_access.html for further details)

Journal of Experimental Botany
www.jxb.oxfordjournals.org

RESEARCH PAPER

Induced epidermal permeability modulates resistance and susceptibility of wheat seedlings to herbivory by Hessian fly larvae

Christie E. Williams[1,2,*], Jill A. Nemacheck[1,2], John T. Shukle[2], Subhashree Subramanyam[3], Kurt D. Saltzmann[2] and Richard H. Shukle[1,2]

[1] USDA-ARS Crop Production and Pest Control Research Unit, MWA, West Lafayette, IN 47907, USA
[2] Department of Entomology, Purdue University, West Lafayette, IN 47907, USA
[3] Department of Agronomy, Purdue University, West Lafayette, IN 47907, USA

* To whom correspondenc should be addressed. E-mail: Christie.Williams@ars.usda.gov

Received 2 December 2010; Revised 18 April 2011; Accepted 26 April 2011

Abstract

Salivary secretions of neonate Hessian fly larvae initiate a two-way exchange of molecules with their wheat host. Changes in properties of the leaf surface allow larval effectors to enter the plant where they trigger plant processes leading to resistance and delivery of defence molecules, or susceptibility and delivery of nutrients. To increase understanding of the host plant's response, the timing and characteristics of the induced epidermal permeability were investigated. Resistant plant permeability was transient and limited in area, persisting just long enough to deliver defence molecules before gene expression and permeability reverted to pre-infestation levels. The abundance of transcripts for GDSL-motif lipase/hydrolase, thought to contribute to cuticle reorganization and increased permeability, followed the same temporal profile as permeability in resistant plants. In contrast, susceptible plants continued to increase in permeability over time until the entire crown of the plant became a nutrient sink. Permeability increased with higher infestation levels in susceptible but not in resistant plants. The ramifications of induced plant permeability on Hessian fly populations are discussed.

Key words: Cuticle, epidermal permeability, GDSL-motif lipase/hydrolase, Hessian fly, wheat, infestation level, neutral red, resistance, susceptibility.

Introduction

As the first line of defence against biotic and abiotic stressors that impact the leaf, the epidermal cell layer is fortified to maintain structural integrity. In many plants, the external surface of the epidermal cell wall is thickened (Evert, 2006), increasing tensile strength (Kutschera, 2008), and is coated with a cuticle that protects against water loss (Schönherr, 1982) while providing defence against pathogens (Kolattukudy, 1985) and insects (Eigenbrode, 1996). Yet the epidermis also exhibits the seemingly incompatible property of limited permeability, allowing for deposition of surface wax and cutin, the two-way exchange of gasses and nutrients, as well as delivery of defence molecules when attacked (reviewed by Javelle *et al.*, 2011).

Temporal changes in leaf epidermal permeability can occur due to both endogenous and environmental factors. Developmentally regulated permeability occurs in leaves of the carnivorous plant *Roridula dentate*, extending through the epidermis to the mesophyll cells and along sclerenchyma surrounding vascular bundles (Anderson, 2005), and may aid in the secretion of digestive enzymes and absorption of nutrients. Leaf permeability can also be altered by disease. Epiphytic bacteria on the ivy *Hedra helix* cause increased outward flow of leaf fluids carrying inorganic and organic molecules that enhance bacterial growth (Schreiber *et al.*, 2005). Virulent Hessian fly larvae [*Mayetiola destructor* (Say)] also cause increased epidermal permeability in their

host wheat plants (*Triticum aestivum* L.) (Shukle *et al.*, 1992) as compatible interactions lead to down-regulation of several wheat genes involved in maintenance of the cuticle and cell wall (Kosma *et al.*, 2010).

For neonate Hessian fly larvae to survive to adulthood, they must be able to induce susceptibility in their host plant, resulting in a compatible interaction. Following egg hatch on the leaf blade, Hessian fly larvae crawl to the base of the plant within the whorl of developing leaves (McColloch, 1923). The tissue in this crown region of the plant where the larvae reside is in the tender elongation zone of the developing leaf where cell walls are plastic to accommodate growth, and layers of cutin and wax, constituting the protective cuticle, are thinnest (Richardson *et al.*, 2007). The extremely minute mandibles of Hessian fly larvae are not structured for chewing (Hatchett *et al.*, 1990), but produce shallow punctures on the leaf surface (Harris *et al.*, 2010). The application of salivary secretions reprogrammes the plant to increase production of nutrients that are beneficial to larvae, including free amino acids (Saltzmann *et al.*, 2008), proteins (Shukle *et al.*, 1992), and sugars (Refai *et al.*, 1955). Rapid changes in surface wax composition and degradation of cutin monomers (Kosma *et al.*, 2010), plus thinning and lysis of epidermal cell walls (Harris *et al.*, 2006) and increased cell permeability (Shukle *et al.*, 1992), result in diffusion of nutrients to the leaf surface during early stages of the interaction. These virulent larvae are thought to simply suck up nutrients that seep out of the epidermal cells once susceptibility is induced (Heath, 1961; Harris *et al.*, 2006). Leaf elongation slows to a halt (Cartwright *et al.*, 1959) and, after several days, the formation of nutritive tissue, similar to the inside surface of a gall, begins to provide sustained nourishment for developing larvae (Harris *et al.*, 2006).

Incompatible interactions occur when attack by Hessian fly larvae triggers defence responses that render the host plant resistant. The resulting gene-for-gene recognition (Hatchett and Gallun, 1970) of larval salivary components initiates chemical (Sardesai *et al.*, 2005) and physical defences (Kosma *et al.*, 2010). Resistant plant surface waxes increase 3-fold and cutin monomer abundance is maintained (Kosma *et al.*, 2010), as cell lysis and the formation of nutritive tissue are blocked (Harris *et al.*, 2010). Soon after resistance is induced, the plants produce lectins with insecticidal properties, which are consumed by the larvae (Giovanini *et al.*, 2007; Subramanyam *et al.*, 2008), and reactive oxygen species are generated (Liu *et al.*, 2010), yet the plants have little or no hypersensitive response (Giovanini *et al.*, 2006). The defence response lasts only 2–3 d and quickly returns to pre-infestation levels (Subramanyam *et al.*, 2008).

The intricate details of wheat interactions with Hessian fly larvae, described above, are important to the study of larval-induced wheat permeability addressed in the current study. Here results of neutral red staining and quantitative real-time PCR (qRT-PCR) studies that addressed three hypotheses are presented: (i) Hessian fly-induced resistance and susceptibility in wheat both involve an increase in epidermal cell permeability; (ii) permeability increases with higher infestation levels; and (iii) the spread of permeability initiated by virulent larvae explains the previously reported rescue of co-infesting avirulent larvae on the same plant.

Materials and methods

Plant care and infestations

Near-isogenic wheat lines, *H9*-Iris (containing the *H9* Hessian fly resistance gene) and Newton (lacking a resistance gene), were used for all experiments. Ten to 15 seeds were sown per 10 cm pot containing Promix Professional growing medium (Premier Horticulture Inc., Quakertown, PA, USA) with time-release fertilizer (18:6:12, ferti-lome Start-N-Grow, Bonham, TX, USA) and covered with vermiculite (Packaging Industries, Inc., North Bloomfield, OH, USA) to ease removal of plants for dissection. After planting, pots were watered and moved to a 4 °C chamber for 1 week to encourage uniform germination. Pots were then transferred to a Conviron growth chamber (Controlled Environments Ltd, Winnipeg, Manitoba, Canada) set at 18 °C and 60% humidity with a 14 h photoperiod for permeability studies. To avoid light-induced alterations in expression of light-responsive genes, which could mask the response of those genes to Hessian fly infestation and confound quantification by qRT-PCR, a 24 h photoperiod was used for qRT-PCR tissues (irradiance 980–1470 μmol m^{-2} s^{-1}.

Hessian fly Biotype L flies (virulent on Newton and avirulent on *H9*-Iris) and *vH9* flies (virulent on *H9*-Iris) were maintained as purified laboratory stocks in a 4 °C cold chamber at the USDA-ARS Crop Production and Pest Control Research Unit at Purdue University, following methods of Sosa and Gallun (1973). When wheat seedlings reached the one-leaf stage, pots were covered with vented plastic cups and infested with four or five mated female flies. After 6 h, flies were removed, resulting in an average of 14 larvae per plant for permeability studies or 18 larvae per plant for qRT-PCR tissues. A range of infestation levels was obtained by infesting with 1–4 mated females which were removed after 2, 4, or 6 h. Uninfested controls received no flies, but were treated in the same way. Pots remained covered until eggs hatched. Eggs were deposited on the blade of the first leaf and larvae fed on the abaxial surface of the developing second leaf. To verify the wheat–Hessian fly interaction, 10 plants per treatment were selected randomly, 3 weeks after infestation, and measured to confirm stunting in the compatible interactions and normal growth in the incompatible interaction and control.

Neutral red staining

When tissues are soaked in solutions of neutral red, this small molecule (axial radii equal to 7.4×3.45×1.9 $Å^3$ with a hydrodynamic volume of 171 $Å^3$; Singh, 2000) is absorbed through discontinuities in the cell surface and causes tissues to take on red colouration. Joel and Juniper (1982) used neutral red staining to distinguish intact plant tissue, which did not absorb stain, from tissue containing cuticular gaps, which did absorb stain. Although the amount of neutral red stain that was absorbed was not quantified in this study, it was presumed that tissues that appeared darker red had absorbed more of the stain, and thus were more permeable, than tissues that appeared lighter in colour.

Roots from wheat seedlings were exposed and cut 1 cm below the root–crown junction. The first leaf was peeled off in strips to avoid wounding the underlying tissue. The basal 2 cm of leaf 2 contained larval feeding sites; therefore, the tissue was cut 4–5 cm above the root–crown junction to avoid wounding near the feeding sites. Uninfested seedlings were dissected in the same manner and used as negative controls or as positive wounding controls when poked with a 0.2 mm minuten pin. Tissue samples were soaked in aqueous 0.1% (w/v) neutral red stain (Sigma-Aldrich, St Louis, MO, USA) for 10 min, and then washed until the water ran clear

(Joel and Juniper, 1982). Because Hessian fly larvae were easily dislodged during the staining process, larval locations were marked with a fine-point Sharpie, which did not induce permeability and was retained during staining (Fig. 1A–D). Representative plants were photographed with a Nikon Stereoscope using Spot Advanced Imaging software (Diagnostic Instruments, Inc., Sterling Heights, MI, USA).

To study the effects of the infestation level on permeability, crown tissue was stained 3 days after egg hatch (DAH) from Biotype L-infested *H9*-Iris plants (resistant), *vH9*-infested *H9*-Iris plants (susceptible), and Biotype L-infested Newton plants (susceptible); this experimental design provided (i) comparison of a compatible and incompatible interaction with wheat type held constant, varying only in fly type; and (ii) two different compatible interactions with fly type held constant, varying only in wheat type (two near-isogenic lines). For each treatment, 4–28 plants were stained from each of the following infestation levels: 0, 1, 2–3, 4–10, 11–20, and >20 larvae per plant. This resulted in a total of 17 groups for the study: 15 infested treatments plus a zero-larva control for each wheat type. A subset of plants from each of the above treatments was poked with a minuten pin as positive wounding controls.

To study the time-course of permeability changes throughout Hessian fly larval infestation, *H9*-Iris plants were dissected and stained 2 d after oviposition (before egg hatch) and at 12 h, and 1, 2, 3, 4, 5, 6, 8, 10, and 12 DAH from the following treatment groups: two uninfested plants, two uninfested positive control plants (poked with minuten pin), six Biotype L-infested plants (resistant), and six *vH9*-infested plants (susceptible).

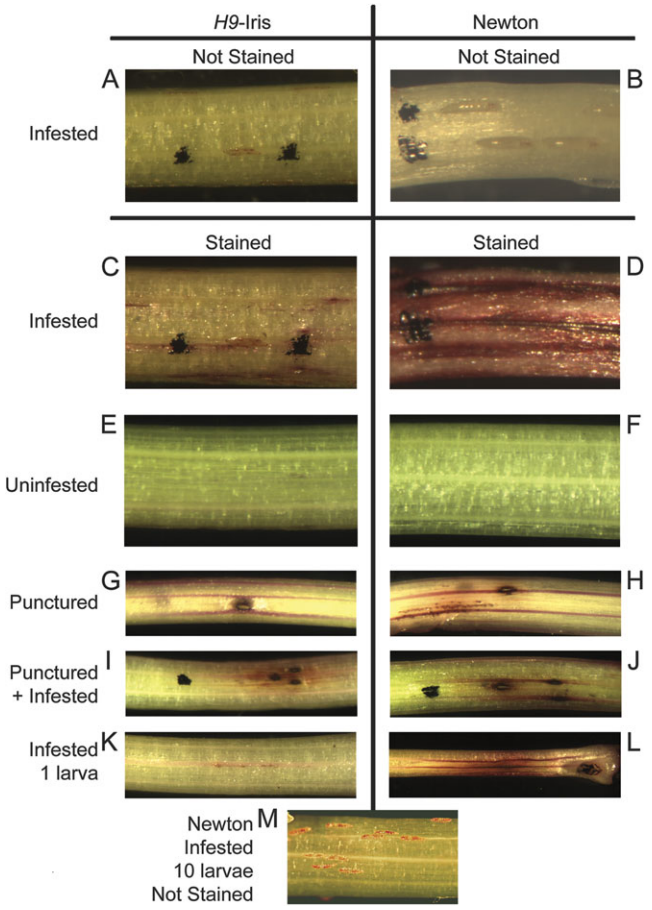

Fig. 1. Controls for induced permeability. *H9*-Iris (resistant) and Newton (susceptible) seedlings received the following treatments before staining with neutral red: infestation with Biotype L Hessian fly larvae that hatched 3 d before staining (A–D; same plants before and after staining), no infestation (E and F), puncturing with a minuten pin (diameter 200 μm) immediately before staining (G and H), puncturing and infestation (I and J), infestation with just one larva per plant (K and L: the length of dark streaks in L is 13.4 mm and the length of one first-instar larva is ~770 μm), and infestation by 10 larvae (M). Seedling diameter is ~2 mm. Black ink from a Sharpie pen was used to mark the locations of larvae (which often dislodged during staining) and punctures, but did not induce permeability. Compatible interactions between *H9*-Iris and *vH9* larvae (not shown) were indistinguishable from compatible interactions between Newton and Biotype L larvae.

Assessment of neutral red staining characteristics

An overall red staining intensity rating scale was established: zero being no staining and seven being a completely red-stained crown (Supplementary Fig. S1 available at *JXB* online). Two plants representing each possible rating were photographed and kept for reference during the scoring process. In addition, plants were given a rating of zero to five for background blush, which was defined as areas of light pink tissue. The numbers of red spots, broken lines, solid lines, and dark streaks (thick solid lines) were counted for each plant (Supplementary Fig. S1). Also, association of marked larval locations with background blush, spots, solid and broken lines, or dark streaks were recorded. Two researchers rated the plants independently and were unaware of the treatment or infestation level. A third person ensured that each scorer rated half of the plants in each treatment group. Four to 28 plants (average=13.6 plants) were scored for each group in the infestation level experiment (e.g. *H9*-Iris infested with 2–3 *vH9* larva per plant) at 3 DAH. Six plants were scored for each time point in the time-course experiment.

Statistical analysis of neutral red staining characteristics

The six neutral red staining characteristics were scaled and centred prior to formal statistical analysis. *H9*-Iris and Newton uninfested control plants grouped together for the final analysis, resulting in 16 groups. Ordination of data for the six scored characteristics (named in Fig. 2) utilized canonical discriminant analysis within the program R (R Development Core Team, 2009) (Fig. 3). Analysis of similarities (ANOSIM) (Clarke and Green, 1988), which is a non-parametric procedure and analogous to a multivariate version of analysis of variance (ANOVA), was conducted using the software PAST (Hammer *et al.* 2001) to determine whether significant differences in the scored staining characteristics existed between plants at various infestation levels (Table 1). Global ANOSIM compared the average ranked euclidean distance between infestation level groups (r_B) with the average ranked euclidean distance within groups (r_W) by the following calculation: $R = \left(r_B - r_W\right) / \left(\frac{n(n-1)}{4}\right)$ where n is the total number of groups. R can vary from –1 (similar samples are all inside the same infestation level groups) to 1 (similar samples are all outside of groups). P-value significance for R was calculated by using 10,000 permutations. Post-hoc pairwise ANOSIMs were calculated between all possible infestation level groups, with a negative value indicating that the two groups were similar and a positive value indicating that they were dissimilar. A step-down sequential Bonferroni correction was applied to significance scores to correct for multiple tests (Table 1). Unpaired Student's *t*-tests were used to analyse select univariate comparisons; corrections for multiple tests were done using the step-down sequential Bonferroni method.

The multivariate canonical discriminant plot (Fig. 3) displays multidimensional data in two-dimensional space. The top and right axes of the plot define the distribution of the points for all 212 plants from the 16 infestation level groups of Table 1, and the

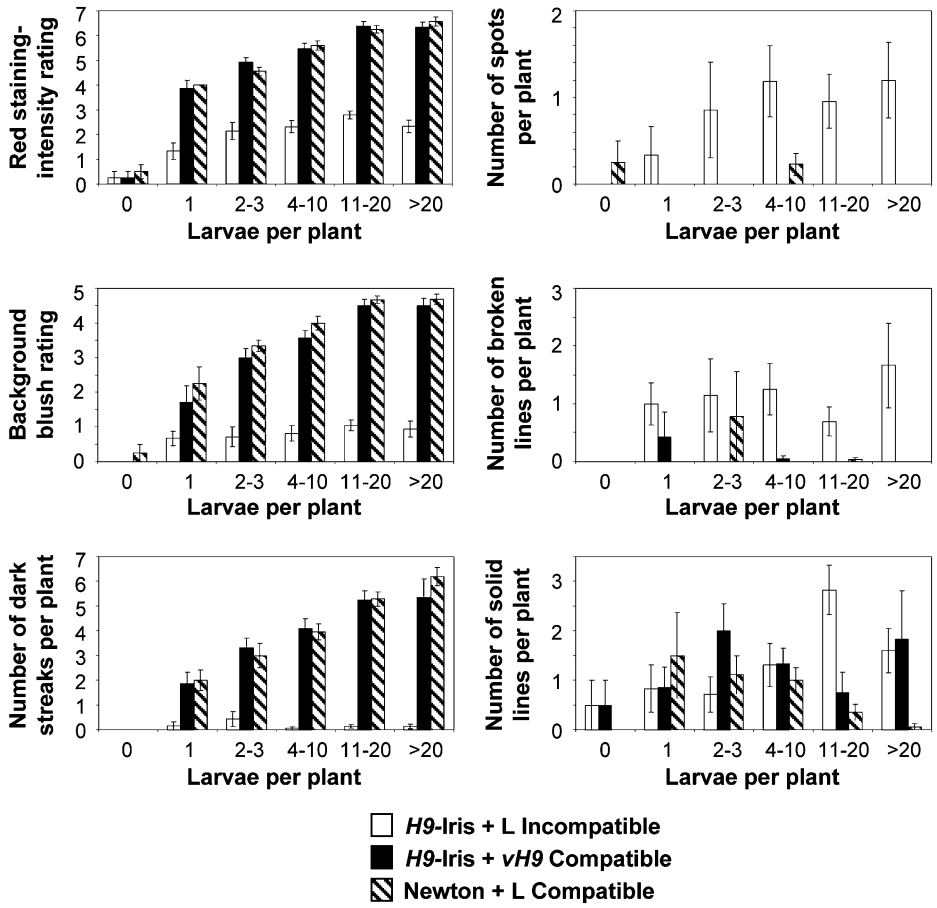

Fig. 2. Effect of the infestation level on rating of six characters associated with permeability. Leaf 3 was stained 3 DAH. The same data set for 212 plants from 16 infestation level groups were analysed in Fig. 2, Fig. 3, and Table 1. Univariant comparisons utilized unpaired Student's *t*-test analysis. Characteristics of neutral red stain absorption were either rated (red staining intensity rating scale from 0 to 7 and background blush rating scale from 0 to 5) or counted (number of dark streaks, spots, broken lines, and solid lines) and then averaged for plants undergoing varying levels of infestation (larvae per plant). Examples of staining intensities in the rating scale are shown in Fig. 1, with ratings of '0' representing plants with no absorbed stain and ratings of '7' (red staining-intensity rating) and '5' (background blush rating) representing plants stained the darkest. White bars correspond to characteristic averages for resistant *H9*-Iris infested with Biotype L larvae (incompatible). Black bars correspond to susceptible *H9*-Iris infested with *vH9* larvae (compatible). Striped bars correspond to susceptible Newton infested with Biotype L larvae (compatible). Standard error of the mean analysis is shown.

centroid for each group is shown within a box. The bottom and left axes define the relationships of the six scored staining characteristics [red staining intensity rating (RR), background blush score (BS), spot count (SC), broken line count (BL), solid line count (SL), and dark streak count (DS)] with regards to canonical axes 1 and 2. The magnitude of effect that each scored character had on the discriminant analysis is proportional to the length of its gradient vector. The position of each plant data point is dictated by the angle and length of the gradient vectors.

Cryosectioning for light microscopy

Following neutral red staining of crown tissues 1, 3, and 7 DAH, 1 cm segments of crown tissue from the base of the wheat plants were cut (25 μm transverse and longitudinal) using a Shandon Cryotome (Thermo Electron Corporation, Pittsburgh, PA, USA), and frozen at –16 °C. Sections were transferred onto microscope slides and mounted in glycerol. These slides were observed under a light microscope and photographed.

Physical measurements

Distances between multiple larvae on the same plant were determined by printing photographs and measuring the distance between anterior ends of every pair of larvae in each of six photographs, which corresponded to six different plants, 28 larvae, and 99 distances between larvae. Dark streak and background blush lengths on plants infested by a single Hessian fly larva, 3 DAH, were determined after neutral red staining by measuring those features on photographs (three biological replicates). The mean distance with the standard error was calculated.

Quantitative real-time PCR (qRT-PCR)

Crown tissue was collected from three biological replicates, each consisting of 32–40 plants of Biotype L-infested resistant *H9*-Iris, Biotype L-infested susceptible Newton, and uninfested control *H9*-Iris and Newton plants at the following time points: 1, 2, 3, 4, 5, and 8 DAH. To isolate the site of larval feeding, the first leaf and any leaves developing internal to leaf sheath 2 were discarded and the bottom 2 cm of the second leaf sheath was harvested. Tissue was immediately frozen in liquid nitrogen and then RNA was isolated using TRIzol reagent (Invitrogen, Carlsbad, CA, USA) according to the manufacturer's protocol.

A probe set sequence on the Affymetrix GeneChip® Wheat Genome Array (Affymetrix Inc., Santa Clara, CA, USA) was

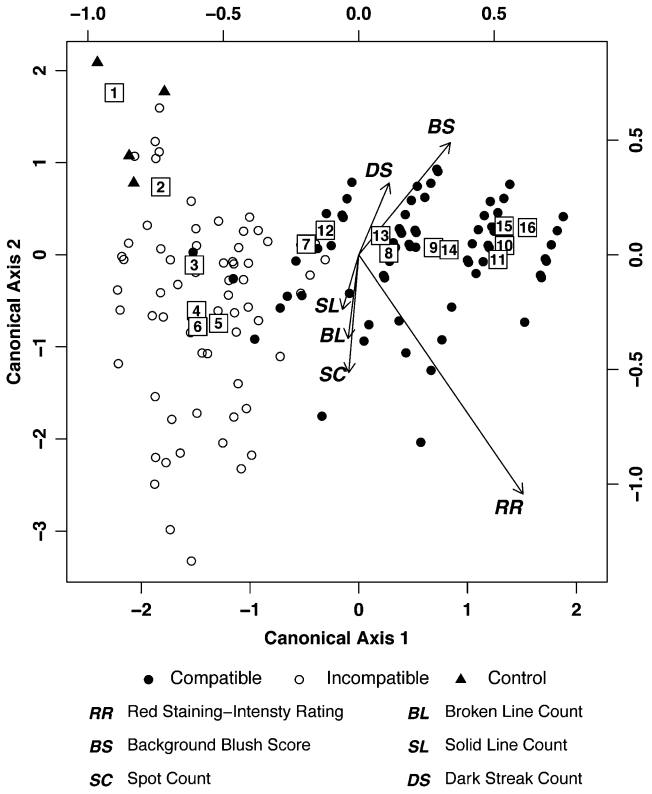

Fig. 3. Multivariate canonical discriminant plot analysis of six characters associated with permeability at different infestation levels. Centroids of the 16 infestation level groups are shown inside boxes marked with the corresponding group numbers from Table 1. Gradient vectors show the relationship of the six scored characteristics [red staining intensity rating (RR), background blush score (BS), spot count (SC), broken line count (BL), solid line count (SL), and dark streak count (DS)] with regards to canonical axes 1 and 2. Data for uninfested control plants are indicated with filled triangles, while data for resistant plants are shown by open circles and for susceptible plants by filled circles. See the Materials and methods for a detailed explanation of the plot.

identified by HarvEST software (http://harvest.ucr.edu; Wheat 1 Array, version 1.54) as annotating to Arabidopsis GDSL-lipase At5g45670. After aligning the probe set sequence to the expressed sequence tag (EST) from which it was derived (CA709446), the overlapping sequence was used for design (Primer Express Software Version 1.5, Applied Biosystems, Foster City, CA, USA) of target-specific primers for amplification of homologous wheat sequences: forward primer CGCCTCTAGTTATGCAACAACCT; reverse primer TGATGATGGATGCGACCTGTA. cDNA synthesis, qRT-PCR analysis, and statistical analyses were performed as reported in Kosma *et al.* (2010).

Results

Characteristics of neutral red staining and effects of infestation level

Plants were stained with neutral red to compare permeability caused by physical damage from a small puncture and permeability caused by the combination of physical damage from larval probing plus chemical damage resulting from salivation. Neutral red stain was absorbed by infested plants but not by uninfested plants (Fig. 1A–F) unless wounded by piercing with a minuten pin, which allowed the stain to enter and spread mainly in major vasculature (Fig. 1G–J). The presence of a single avirulent larva induced changes leading to minimal staining (0.7±0.1 mm in length, n=6) in resistant *H9*-Iris plants (Fig. 1K). Despite the tiny length (2 μm) and diameter (0.2 μm) of larval mandibles that probe the leaf surface (Harris *et al.*, 2010), a single virulent larva was able to induce a larger area of permeability on a susceptible plant (Fig. 1L; dark streak length of 12.5±2 mm and background blush 7.2±0.3 mm, n=3) than was the puncture wound from a 200 μm diameter minuten pin (Fig. 1G, H; dark streak length 1.8±0.2 mm on six plants) used to simulate physical damage from an insect. In infestations with multiple virulent larvae per plant, the average larval length was 0.5±0.01 mm (2 DAH) and the average distance between first-instar larvae at the crown was 1.6±0.1 mm when measured from the anterior end of one larva to the anterior end of each other larva in a photograph (example Fig. 1M). Thus the area of background blush and dark streaking, induced by an individual virulent larva, spread to involve an area of the leaf larger than the 'personal space' between larvae.

A system for rating six characteristics of neutral red stain absorption was established with representative plants (Supplementary Fig. S1 at *JXB* online). The goal was to determine whether resistant plants had smaller neutral red staining features than did susceptible plants, and thus minimized the spread of cell permeability as part of their defence against Hessian fly larvae. Infested susceptible plants stained more darkly than did resistant plants (Fig. 2; red staining intensity rating). Only a small overlap in staining intensity and characteristics was observed between susceptible and resistant plants, as demonstrated by distinct groupings of the 16 infestation level centroids on a canonical discriminant plot (Fig. 3; used same data as in Fig. 2 and Table 1). The distribution of absorbed neutral red stain differed between susceptible and resistant plants. Background blush was more intense and dark streaks were more prevalent features in susceptible plants (Figs. 2, 3), indicating intercellular spread of permeability. In contrast, features with more limited distribution—spots, broken lines, and solid lines—were more common in resistant plants (Figs. 2, 3) (example: significant differences for prevalence of features at the infestation level of 11–20 larvae in *H9*-Iris resistant compared with *H9*-Iris susceptible plants: spots, P=0.030; broken lines, P=0.037; solid lines, P=0.029; *H9*-Iris resistant compared with Newton susceptible plants: spots, P=0.030; broken lines, P=0.035; solid lines, P=0.001).

Previous work (Subramanyam *et al.*, 2008) indicated that virulent larvae quickly settled into permanent feeding sites whereas avirulent larvae moved away from unsuccessful attempted feeding sites. This information prompted the investigation of an association of larval locations with tissue that stained with neutral red. On stained susceptible plants 3 DAH, 20 out of 20 marked larval locations were associated with background blush and dark streaks.

Table 1. Comparison of infestation level groups for staining characteristics associated with wheat cell permeability at 3 DAH

Global ANOSIM

Permutations	Mean rank within groups	Mean rank between groups	*R*	*P*-value
10 000	6812	1.15E-04	0.423	<0.0001

Post-hoc pairwise ANOSIMs[a]

Group	Infestation level	Controls	I+L 1	I+L 2-3	I+L 4-10	I+L 11-20	I+L >20	I+*vH9* 1	I+*vH9* 2-3	I+*vH9* 4-10	I+*vH9* 11-20	I+*vH9* >20	N+L 1	N+L 2-3	N+L 4-10	N+L 11-20	N+L >20
1	Controls		**	**				**	***	***	**	**	**	**	***	***	***
2	I+L 1 larva	**0.38**						*	***	***	**	**	*	**	***	***	***
3	I+L 2–3 larvae	**0.44**	−0.08						***	***	**	**		**	**	***	***
4	I+L 4–10 larvae	0.01	−0.2	−0.14					***	***	***	**		*	***	***	***
5	I+L 11–20 larvae	0.15	−0.03	0.03	0.05				**	***	***	***		*	***	***	***
6	I+L >20 larvae	0.09	−0.13	−0.14	−0.02	0.06			***	***	**	**			***	***	***
7	I+*vH9* 1 larva	**0.76**	**0.35**	0.11	0	0.07	−0.03			*	**	**			**	***	***
8	I+*vH9* 2–3 larvae	**0.83**	**0.67**	**0.57**	**0.46**	**0.31**	**0.37**	0.11							*	***	***
9	I+*vH9* 4–10 larvae	**0.93**	**0.84**	**0.76**	**0.67**	**0.56**	**0.59**	**0.3**	0.06							**	**
10	I+*vH9* 11–20 larvae	**1.0**	**1.0**	**0.83**	**0.64**	**0.61**	**0.42**	**0.68**	0.18	−0.03			**	**			
11	I+*vH9* >20 larvae	**0.99**	**0.95**	**0.75**	**0.63**	**0.56**	**0.37**	**0.58**	0.21	0.13	0		*	*			
12	N+L 1 larva	**0.98**	**0.52**	0.08	−0.03	−0.02	−0.1	−0.17	−0.06	0.24	**0.88**	**0.59**				***	**
13	N+L 2–3 larvae	**0.78**	**0.6**	**0.39**	**0.28**	**0.27**	0.17	0.06	−0.02	0.05	**0.37**	**0.32**	0.01			***	***
14	N+L 4–10 larvae	**0.98**	**0.91**	**0.83**	**0.72**	**0.63**	**0.63**	**0.35**	**0.12**	0	−0.07	0.14	0.29	0.06		*	**
15	N+L 11–20 larvae	**1.0**	**1.0**	**0.97**	**0.88**	**0.83**	**0.83**	**0.77**	**0.47**	**0.21**	−0.04	0.2	**0.83**	**0.52**	**0.13**		
16	N+L >20 larvae	**1.0**	**1.0**	**0.96**	**0.83**	**0.8**	**0.72**	**0.89**	**0.52**	**0.28**	0.12	0.27	**0.95**	**0.71**	**0.19**	−0.03	

*≤0.05; ** ≤0.005; ***<0.0001

[a] Magnitude of similarity (negative value)/dissimilarity (positive value) is given below the diagonal, with significant values in bold. Significance level is indicated above the diagonal. Groups 1–16 correspond to centroids in Fig. 1B. 'I' represents *H9*-Iris plants, 'N' Newton plants, 'L' Biotype L larval infestation, '*vH9*' *vH9* larval infestation. Controls were not infested. All six staining characteristics from Fig. 1A were analysed together to produce the represented values.

Multiple larvae were often lined up along these dark streaks, having established permanent feeding sites directly over major veins in the leaf (example: Fig. 1B, D). In contrast, marked larval locations on resistant plants were associated with stained features only 60% of the time.

Neutral red stain intensity increased with higher infestation levels, regardless of whether the host plants were resistant or susceptible (Fig. 2, red staining intensity rating: example *P*values for 1 versus >20 larvae: *H9*-Iris with Biotype L, $P=0.036$; *H9*-Iris with *vH9*, $P=0.001$; and Newton with Biotype L, $P<0.001$; and Fig. 3 centroid distribution displaying correlation between infestation level and red staining intensity rating RR). However, at each of the five infestation levels, background blush ratings and the number of dark streaks were significantly higher for susceptible plants compared with resistant plants, and these characters became more pronounced with increasing infestation level (Fig. 2, *P*-values for 1 versus >20 larvae: *H9*-Iris with *vH9*, background blush $P=0.005$, dark streaks $P=0.028$; Newton with Biotype L, background blush $P=0.043$, dark streaks $P<0.001$).

Significant differences in staining variation existed among the 16 different infestation level groups when all six scored characteristics (from Fig. 2) were considered together (Table 1; demonstrated by the *R*-value being >0 in the Global ANOSIM). Post-hoc ANOSIMs examining staining variation showed that the rating for one larva per plant significantly differed from that for four or more larvae per plant in susceptible *H9*-Iris infested with *vH9* (Table 1; $R=0.3$, $P=0.009$). Similarly, in susceptible Newton infested with Biotype L, a significant difference was detected between plants hosting 1 versus ⩾11 larvae per plant (Table 1: $R=0.83$, $P<0.0001$). However, for resistant *H9*-Iris plants infested with Biotype L, no significant differences were found between any levels of infestation (Table 1). In addition, post-hoc ANOSIMs found that susceptible plants with two or more larvae were significantly different (darker staining; Fig. 2 red staining intensity rating, and Table 1) from any level of larval infestation in resistant plants (except for N+L 2–3 larvae versus I+L >20, Table 1). Uninfested control plants stained significantly differently (lighter; Fig. 2 red staining intensity rating, and Table 1) from any level of infestation in either of the two genotypes of susceptible plants.

In order to determine whether higher infestation levels on resistant plants resulted in increased scores for the six characteristics, post-hoc ANOSIM was used to compare staining of tissue at various infestation levels with uninfested

control tissue. Control plants stained significantly differently from resistant plants with three or fewer larvae (Table 1; control versus I+L 2–3 larvae: R=0.44, P=0.0003). However, surprisingly, control plants showed no significant difference from resistant plants infested with four or more larvae (Table 1: control versus I+L 4–10 larvae; R=0.01, P=NS).

Effect of duration of infestation on permeability (time-course)

To determine whether increased permeability in susceptible and resistant plants is a permanent and static change, time-course experiments were performed. In both resistant and susceptible wheat plants (average infestation level of 14 larvae per plant), permeability to neutral red stain was evident within 12 h of egg hatch (data not shown). Surprisingly, in resistant plants, less stain was observed 3 and 4 DAH compared with 2 DAH (P=0.0005 and 0.0003, *Fig. 4*).

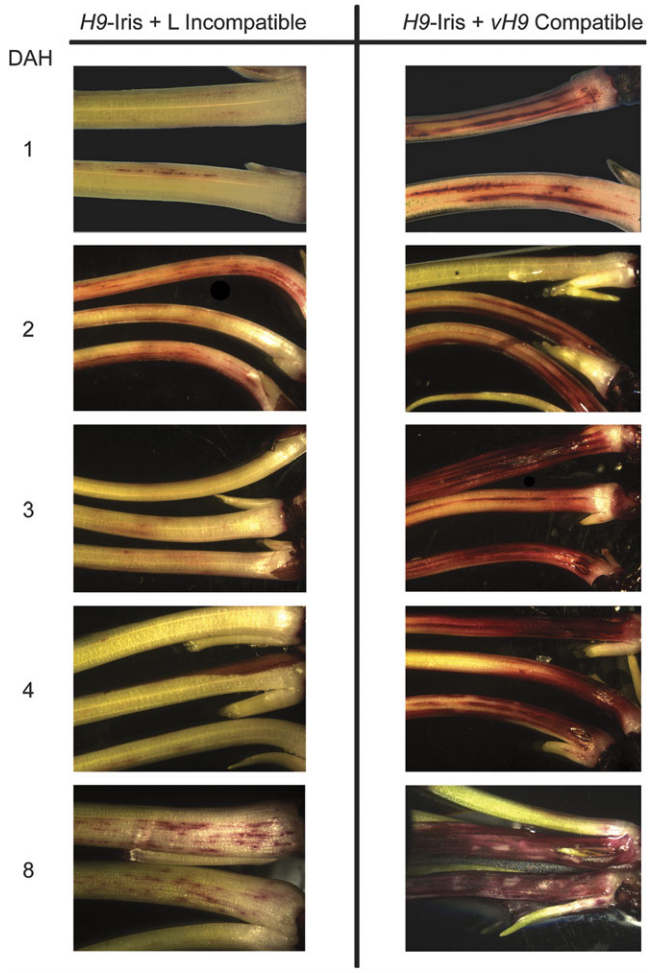

Fig. 4. Changes in plant cell permeability over time. *H9*-Iris seedlings were infested with Biotype L (resistant plant/avirulent larvae/incompatible interaction) or *vH9* Hessian fly (susceptible plant/virulent larvae/compatible interaction). Plant tissues were harvested after 12 h and at 1, 2, 3, 4, 5, 6, 8, 10, and 12 DAH. Examples from 12 h and days 5, 6, 10, and 12 are not shown. After removal of the outer leaf, the tissues were stained with neutral red. Seedling diameter is ~1.5 mm at 1 DAH and 2.5 mm at 8 DAH.

In contrast, the susceptible plants stained more heavily as time progressed (Fig. 4), with dark red staining around the entire circumference of the crown by 3 DAH. By 8 DAH and until the end of the experiment at 12 DAH, all larvae were dead on resistant plants, and localized patches of stained tissue were seen, whereas second-instar larvae were present on susceptible plants that stained intensely (Fig. 4).

Cellular localization of neutral red stain

To determine which tissues and cells types within the crown increased in permeability, microscopy studies were conducted. Neutral red-stained wheat crown tissues were frozen and sliced into 25 μm thick transverse (Supplementary Fig. S2 at *JXB* online) and longitudinal sections (Supplementary Fig. S3). At 1 DAH, differences in staining intensity or location were indistinguishable in transverse sections of resistant and susceptible plants; staining was localized to a few of the epidermal cells and the vascular bundles of the second leaf sheath. However, by 3 DAH susceptible plants stained more intensely, in epidermal cells, vascular tissues, and some of the mesophyll cells of the second leaf, than did the resistant plants where the red stain was restricted to some of the epidermal cells and vascular bundles. By 7 DAH, transverse sections of susceptible plants revealed additional staining in cells of the interior developing third leaf. In contrast, resistant plants at 7 DAH showed a reduced level of staining, restricted to the epidermal layer, and the intensity of staining was less than on 1 DAH. The uninfested Iris and Newton control plants did not absorb stain at any of the time points. Longitudinal sections revealed staining patterns similar to those of transverse sections.

Increased abundance of GDSL-motif lipase/hydrolase mRNA

Previous work demonstrated that several known mechanisms believed to increase cell permeability were operational in susceptible but not in resistant wheat plants during Hessian fly attack (Kosma *et al.*, 2010). However, through qRT-PCR, at 1 DAH in resistant plants a sudden 51-fold increase (P=0.00003) was identified in GDSL-motif lipase/hydrolase mRNA (Fig. 5) encoding an enzyme thought to alter cutin organization and increase cuticular permeability (Yeats *et al.* 2010). The abundance of this transcript decreased rapidly, paralleling the temporal profile of transient permeability in resistant wheat cells during larval attack. No significant increase in the abundance of this message was detected in susceptible plants.

Discussion

The goal of this study was to gain insight into spatial and temporal aspects of wheat nutrient and defence molecule delivery to Hessian fly larvae during the first few days of attack. After staining with neutral red, changes in permeability became apparent in epidermal cells on the abaxial surface of developing wheat leaves hosting larvae. Through

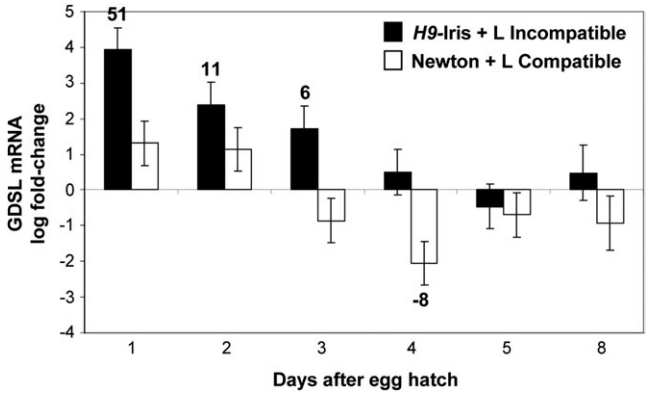

Fig. 5. Influence of Hessian fly larvae on wheat GDSL-lipase (EST CA709446) mRNA abundance. Transcript levels were quantified by qRT-PCR in samples from developing leaf tissue at the crown of seedlings involved in incompatible (resistant *H9*-Iris wheat infested with Biotype L larvae; black bars) and compatible (susceptible Newton wheat infested with Biotype L larvae; white bars) interactions or from uninfested control plants (baseline of 0). Bars represent log fold change ±SE of infested samples with respect to uninfested controls. Numbers above or below bars indicate non-log fold change in samples showing significant differences from control levels (P <0.05). The experiment was conducted with three biological replicates each subjected to qRT-PCR three times (three technical replicates).

this process it was possible to test three hypotheses that were unanswered by previous research.

Hypothesis 1

Hessian fly-induced resistance and susceptibility in wheat both involve an increase in epidermal cell permeability. Although permeability in susceptible plants was noted previously (Shukle *et al.*, 1992), increased permeability was also expected as resistance became established. This expectation was based on previous work showing that within a few hours of attack, avirulent Hessian fly larvae ingest wheat lectins, but these molecules lack a signal sequence (Giovanini *et al.*, 2007; Subramanyam *et al.*, 2008), which is necessary to target proteins for secretion (Gang *et al.*, 1999). Since Hessian fly larvae are small with non-chewing mouthparts that may not be able to penetrate the entire thickness of the cell wall at the leaf surface (Harris *et al.*, 2010), the plant must be able to deliver defence molecules by some passive mechanism such as diffusion through permeable tissue. Neutral red staining verified that developing leaves of resistant wheat plants involved in incompatible interactions became more permeable as expected (Figs 1C, K, 2, 4), even though genes responsible for maintaining surface integrity are not down-regulated as they are in susceptible plants (Kosma *et al.*, 2010). Instead, the abundance of GDSL-motif lipase/hydrolase mRNA increased 51-fold in resistant plants (Fig. 5), suggesting an alternative mechanism of permeability that avoids destruction of the leaf surface. A proposed function of a similar GDSL-motif lipase/hydrolase gene in tomato fruit is the loosening and realignment of cutin to allow cuticle reorganization during growth (Yeats *et al.*, 2010). Increased permeability can facilitate resistance to pathogens, as demonstrated in studies of *Arabidopsis bre 1* mutants that are more resistant to *Botrytis* due to permeability-enhanced plant detection of fungal effectors and increased delivery of anti-fungal compounds to the leaf surface (Bessire *et al.*, 2007). Remodelling of the cuticle has been documented in other plants, including temporal changes in leaf permeability in some carnivorous plants through the formation of cuticular gaps, pores, and discontinuities caused by selective deposition and breakdown of cutin (Joel and Juniper, 1982). Thus changes in epidermal permeability are common during the lifetime of a leaf (Schreiber *et al.*, 2005) and facilitate the exchange of molecules between plants and their environment.

The wheat cells involved in defence molecule export were expected to be in small clusters. This expectation was based on previous work showing that during dual infestation, when virulent larvae hatch before (Grover *et al.*, 1989) or up to a few days after resistance has been induced (SD Baluch and CE Williams, unpublished results) by avirulent larvae, both types of larvae are able to feed and survive. It was presumed that these larvae survived on a plant that was expressing induced resistance because areas of resistant tissue were small, so the larvae could move to adjacent tissue on the same leaf that was not producing defence molecules and the virulent larvae could then induce that tissue to become susceptible. The results showed that resistant plants infested with a single larva did respond with small regions of permeability (the average length of stainable tissue was 0.7 mm; Fig. 1K) compared with the extensive regions detected in susceptible plants infested with only one larva (dark streak length 12.5 mm and background blush length 7.2 mm; Fig. 1L). In addition, only 60% of the avirulent larvae on resistant plants were associated with the small stained features, indicating that they were able to migrate away from the regions of permeability. Microscopy studies showed that permeability in resistant plants was limited to a few epidermal cells and vascular bundles (Supplementary Figs S2, S3 at *JXB* online). Finally, the duration of permeability in resistant plants was short, with the largest stainable areas visible 2 DAH (Fig. 4), which corresponded to the peak expression of several defence genes (Sardesai *et al.*, 2005; Subramanyam *et al.*, 2008; Liu *et al.*, 2010; Fig. 6), and returned to near-control levels of permeability and gene expression by 4 DAH. By this stage of the resistance response, the outer wall of epidermal cells at larval feeding sites has begun to thicken (Harris *et al.*, 2010), creating a structural barrier and causing additional rigidity that could contribute to the small decrease in the rate of leaf expansion that was noted by Anderson and Harris (2008). In addition, subcellular changes associated with penetration resistance mechanisms, such as more abundant organelles, have begun to develop (Anderson and Harris, 2010). It appears from the current study, as well as histological studies of resistant plant cells responding to Hessian fly attack (Harris *et al.* 2010), that induced responses are of short duration and limited to a small

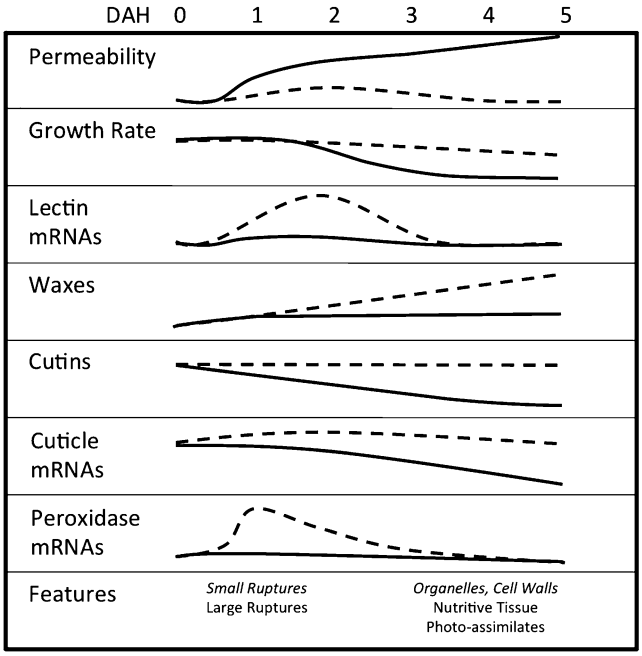

Fig. 6. Summary of trends over time for the wheat leaf hosting Hessian fly larvae in resistant and susceptible plants. Information about incompatible interactions (resistant wheat and avirulent larvae) is shown by dashed lines and italic text, and information about compatible interactions (susceptible plants and virulent larvae) is show by solid lines and Roman text. Data are summarized from the following: changes in permeability, this study; changes in leaf growth rate, Anderson and Harris (2008); abundance of lectin mRNAs, Subramanyam *et al.* (2006) and Giovanini *et al.* (2007); abundance of waxes, cutins, and mRNAs encoding proteins involved in maintenance of cuticle integrity, Kosma *et al.* (2010) and Saltzmann *et al.* (2010); abundance of peroxidase mRNAs encoding proteins that produce reactive oxygen species in plant defence, Liu *et al.* (2010); timing of appearance of features including epidermal ruptures, abundance of organelles (endoplasmic reticulum, small vesicles), increase in epidermal cell wall thickness, development of nutritive tissue, and diversion of photo-assimilates to the nutritive tissue, Harris *et al.* (2006, 2010).

area. This means that resistance costs the plant very little: seedlings show only minor growth deficits (Anderson and Harris, 2006, 2008) and mature plants exhibit no yield penalties or quality problems (Anderson *et al.*, 2011).

Although Hessian fly-induced permeability of susceptible plants was reported previously (Shukle *et al.*, 1992), the present time-course experiment (Fig. 4) demonstrated the spatial progression and timing related to other events known to occur as susceptibility progresses (Fig. 6). Initially, at 1 DAH, permeability visualized by neutral red staining was most pronounced in longitudinal streaks associated with the location of larvae, suggesting the translocation of a signal through the vasculature of the plant. During this period, expression of genes associated with susceptibility (Puthoff *et al.*, 2005) and amino acid production (Saltzmann *et al.*, 2008) has already increased, and expression of genes associated with maintaining epidermal integrity (Kosma *et al.*, 2010; Saltzmann *et al.*, 2010) has begun to decrease. At 2 DAH, involvement of tissue between the major veins of the leaf was apparent (Fig. 4), corresponding to a significant decrease in the rate of growth for the leaf hosting the virulent larvae compared with controls or plants hosting avirulent larvae (Anderson and Harris, 2008). This correlation is noteworthy because an intact epidermis is essential to maintain the turgor that is required to power leaf growth in the zone of cell elongation (Kutschera, 2008; Javelle *et al.*, 2011), which is where Hessian fly larvae feed. By 4 DAH extensive background blush is visible in stained susceptible plants. At this time, the nutritive tissue that sustains the developing larvae has been established (Harris *et al.*, 2008).

Hypothesis 2

Permeability increases with higher infestation levels. It was expected that the permeability induced by a single virulent larva would be more extensive than that caused by disruption from a small wound (simulating mechanical damage from mandibles of a larva) because it is believed that the larval saliva contains effectors that elicit changes in the physiology of the host plant. The results documenting the length of permeable regions supported this expectation. Since only one virulent larva is required to induce susceptibility in a plant (Grover *et al.*, 1989), it was not surprising that at all infestation levels, three of the characters used to assess permeability resulted in higher scores for susceptible plants than for uninfested controls or resistant plants (Fig. 2). In addition, at higher infestation levels, susceptible plants would receive more saliva from virulent feeding larvae, leading to scores that increased with infestation level for three of the characters used to assess permeability (Fig. 2). These results fit well with previous work showing that the expression of some genes is responsive to the infestation level (Giovanini *et al.*, 2007; Saltzmann *et al.*, 2010). Higher infestation led to only slightly higher scores for resistant plants, perhaps because avirulent larvae are deterred from feeding and continue roaming (Subramanyam *et al.*, 2008) and thus would not apply comparable quantities of saliva to the plant.

Hypothesis 3

The spread of permeability initiated by virulent larvae explains the previously reported rescue of co-infesting avirulent larvae on the same plant. Work by Grover *et al.* (1989) yielded surprising results showing that both virulent and avirulent Hessian fly larvae survive when they reside together on the same wheat plant. It was further demonstrated that when avirulent larvae hatch a few days before virulent larvae, both are able to survive even though plant resistance has been induced (SD Baluch and CE Williams, unpublished results). The survival of both virulent and avirulent larvae during dual infestations may be due to the different spatial and temporal characteristics of resistant versus susceptible permeability. Although first-hatching avirulent larvae would initiate resistance before co-infesting

virulent larvae hatch, the permeability that is believed to be responsible for delivering defence molecules during resistance is localized to small clusters of cells and is of short duration, leaving surrounding areas largely unaffected. Avirulent larvae can escape to these unaffected areas because they do not die immediately, but survive for several days after resistance is initiated (Gallun, 1977) and continue to roam (Subramanyam *et al.*, 2008) without feeding (Gallun and Langston, 1963). Once even a single virulent larva initiates susceptibility, avirulent larvae are able to survive (Grover *et al.*, 1989). It was shown here that a single virulent larva caused cell permeability to spread ~3.6 mm both anterior and posterior to its feeding site (Fig. 1L), which is greater than the average distance of 1.6 mm between first-instar larvae at the crown (Fig. 1M). Thus susceptible permeability spreads outward from the location of virulent larvae and could develop beneath nearby avirulent larvae, allowing them to survive. Susceptible permeability increased with higher infestation levels, ultimately involving a large area of the leaf capable of supporting many virulent and avirulent larvae. Because field infestations consist of Hessian fly populations segregating for multiple virulence/avirulence genes and alleles (Ratcliffe *et al.*, 2000), dual infestations can occur when a mixture of virulent and avirulent eggs are deposited by two different females or by a female that is heterozygous for virulence. An expected outcome of the obviation of resistance resulting from dual infestation is that more avirulent larvae would mature to adulthood and Hessian fly diversity would be enhanced in field populations, resulting in lower selection pressure than if dual infestations did not occur.

In conclusion, this study suggests that although both resistant and susceptible wheat plants increase in epidermal permeability soon after Hessian fly larvae begin to probe, the mechanisms and duration of permeability differ. This permeability may allow salivary effectors to enter plant cells and induce resistance or susceptibility. Susceptible plant permeability may be essential for nutrient delivery that sustains larvae until the establishment of nutritive tissue. Resistant plant permeability appears to be maintained just long enough to deliver defence molecules before it is repaired. Thus resistance is localized and transient, while susceptibility is global. Increases in infestation level have a more pronounced effect on the spread of permeability in susceptible than in resistant plants. The three-dimensional spread of susceptible permeability could account for rescue of avirulent larvae during dual infestation with virulent larvae. Thus a dual-infested plant could act as a refuge for avirulent larvae, maintaining them in the population and effectively decreasing selection pressure.

Supplementary data

Supplementary data are available at JXB online.

Figure S1. Scoring for plant cell permeability.

Figure S2. Cell permeability in transverse sections.

Figure S3. Cell permeability in longitudinal sections.

Acknowledgements

This is a joint contribution by the USDA Agricultural Research Service and Purdue University. We would like to thank Sue Cambron (USDA-ARS) for maintaining Hessian fly stocks, Debra Sherman (Purdue) for use of the Life Science Microscopy Facility, and Carol Sousa (Bone and Articulation Research Laboratory, Purdue) for assistance with cryosectioning. Research was supported by USDA CRIS number 3602-22000-016-D. Mention of trade names or commercial products in this publication is solely for the purpose of providing specific information and does not imply recommendation or endorsement by the US Department of Agriculture. USDA is an equal opportunity provider and employer.

References

Anderson B. 2005. Adaptations to foliar absorption of faeces: a pathway in plant carnivory. *Annals of Botany* **95,** 757–761.

Anderson KG, Harris MO. 2008. Leaf growth signals the onset of effective plant resistance against Hessian fly larvae. *Entomologia Experimentalis et Applicata* **128,** 184–195.

Anderson KG, Harris MO. 2006. Does r-gene resistance allow wheat to prevent plant growth effects associated with Hessian fly (Diptera: Cecidomyiidae) attack? *Journal of Economic Entomology* **99,** 1842–1853.

Anderson KM, Kang Q, Reber J, Harris MO. 2011. No fitness cost for wheat's *H*-gene mediated resistance to Hessian fly (Diptera: Cecidomyiidae). *Journal of Economic Entomology* (in press).

Bessire M, Chassot C, Jacquat AC, Humphry M, Borel S, Petetot JMC, Metraux JP, Nawrath C. 2007. A permeable cuticle in *Arabidopsis* leads to a strong resistance to *Botrytis cinerea*. *EMBO Journal* **26,** 2158–2168.

Cartwright WB, Caldwell RM, Compton LE. 1959. Responses of resistant and susceptible wheats to Hessian fly attack. *Agronomy Journal* **51,** 529–531.

Clarke KR, Green RH. 1988. Statistical design and analysis for a 'biological effects' study. *Marine Ecology Progress Series* **46,** 213–226.

Eigenbrode SD. 1996. Plant surface waxes and insect behaviour. In: Kerstiens G, ed. *Plant cuticles: an integrated functional approach*. Oxford: BIOS Scientific Publishers, 201–222.

Evert RF. 2006. Epidermis. In: *Esau's plant anatomy: meristems, cells, and tissues of the plant body: their structure, function, and development*, 3rd edn. Hoboken, NJ: John Wiley & Sons Inc., 211–254.

Gallun RL. 1977. Genetic basis of Hessian fly epidemics. *Annals of the New York Academy of Sciences* **287,** 223–229.

Gallun RL, Langston R. 1963. Feeding habits of Hessian fly larvae on ^{32}P-labeled resistant and susceptible wheat seedlings. *Journal of Economic Entomology* **56,** 702–706.

Gang DR, Kasahara H, Xia ZQ, Mijnsbrugge KV, Baun G, Boerjan W, Montagu MV, Davin LB, Lewis NG. 1999. Evolution of plant defense mechanisms: relationships of phenylcoumaran benzylic

ether reductases to pinoresinol-lariciresinol and isoflavone reductases. *Journal of Biological Chemistry* **274,** 7516–7527.

Giovanini MP, Puthoff DP, Nemacheck JA, Mittapalli O, Saltzmann KD, Ohm HW, Shukle RH, Williams CE. 2006. Gene-for-gene defense of wheat against the Hessian fly lacks a classical oxidative burst. *Molecular Plant-Microbe Interactions* **19,** 1023–1033.

Giovanini MP, Saltzmann KD, Puthoff DP, Gonzalo M, Ohm HW, Williams CE. 2007. A novel wheat gene encoding a putative chitin-binding lectin is associated with resistance against Hessian fly. *Molecular Plant Pathology* **8,** 69–82.

Grover PBJ, Shukle RH, Foster JE. 1989. Interactions of Hessian fly (Diptera: Cecidomyiidae) biotypes on resistant wheat. *Environmental Entomology* **18,** 687–690.

Hammer Ø, Harper DAT, Ryan PD. 2001. PAST: Paleontological Statistics Software Package for Education and Data Analysis. *Palaeontologia Electronica* **4,** (9) .http://palaeo-electronica.org/2001_1/past/issue1_01.htm.

Harris MO, Freeman TP, Moore JA, Anderson KG, Payne SA, Anderson KM, Rohfristsch O. 2010. H-gene-mediated resistance to Hessian fly exhibits features of penetration resistance to fungi. *Phytopathology* **100,** 279–289.

Harris MO, Freeman TP, Rohfritsch O, Anderson KG, Payne SA, Moore JA. 2006. Virulent Hessian fly (Diptera: Cecidomyiidae) larvae induce a nutritive tissue during compatible interactions with wheat. *Arthropod Biology* **99,** 305–316.

Hatchett JH, Gallun RL. 1970. Genetics of the ability of the Hessian fly, *Mayetiola destructor*, to survive on wheats having different genes for resistance. *Annals of the Entomological Society of America* **63,** 1400–1407.

Hatchett JH, Kreitner GL, Elzinga RJ. 1990. Larval mouthparts and feeding mechanism of the Hessian fly (Diptera: Cecidomyiidae). *Annals of the Entomological Society of America* **83,** 1137–1147.

Heath GW. 1961. An investigation into leaf deformation in *Medicago sativa* caused by the gall midge *Jaapiella medicaginis* Rübs. (Cecidomyiidae). *Marcellia* **30,** 185–199.

Javelle M, Vernoud V, Rogowsky PM, Ingram GC. 2011. Epidermis: the formation and functions of a fundamental plant tissue. *New Phytologist* **189,** 17–39.

Joel DM, Juniper BE. 1982. Cuticular gaps in carnivorous plant glands. In: Cutler DF, Alvin KL, Price CE, eds. *The plant cuticle.*. London: Academic Press, 121–130.

Kolattukudy PE. 1985. Enzymatic penetration of the plant cuticle by fungal pathogens. *Annual Review of Phytopathology* **23,** 223–250.

Kosma DK, Nemacheck JA, Jenks MA, Williams CE. 2010. Changes in properties of wheat leaf cuticle during interactions with Hessian fly. *The Plant Journal* **63,** 31–43.

Kutschera U. 2008. The growing outer epidermal wall: design and physiological role of a composite structure. *Annals of Botany* **101,** 615–621.

Liu XM, Williams CE, Nemacheck JA, Wang H, Subramanyam S, Zheng C, Chen MS. 2010. Reactive oxygen species are involved in plant defense against a gall midge. *Plant Physiology* **152,** 985–999.

McColloch JW. 1923. The Hessian fly in Kansas. *Kansas Agricultural Experiment Station Bulletin 11* .

Puthoff DP, Sardesai N, Subramanyam S, Nemacheck JA, Williams CE. 2005. *Hfr-1*, a wheat cytolytic toxin-like gene, is up-regulated by virulent Hessian fly larval feeding. *Molecular Plant Pathology* **6,** 411–423.

R Development Core Team. 2009. R: a language and environment for statistical computing. R Vienna, Austria: Foundation for Statistical Computing. http://www.R-project.org.

Ratcliffe RH, Cambron SE, Flanders KL, Bosque-Perez NA, Clement SL, Ohm HW. 2000. Biotype composition of Hessian fly (Diptera: Cecidomyiidae) populations from the southeastern, midwestern and northwestern United States and virulence to resistance genes in wheat. *Journal of Economic Entomology* **93,** 1319–1328.

Refai FY, Jones ET, Miller BS. 1955. Some biochemical factors involved in the resistance of the wheat plant to attack by the Hessian fly. *Cereal Chemistry* **32,** 437–442.

Richardson A, Wojciechowski T, Franke R, Schreiber L, Kerstiens G, Jarvis M, Fricke W. 2007. Cuticular permeance in relation to wax and cutin development along the growing barley (*Hordeum vulgare*) leaf. *Planta* **225,** 1471–1481.

Saltzmann KD, Giovanni MP, Ohm HW, Williams CE. 2010. Transcript profiles of two wheat lipid transfer protein-encoding genes are altered during attack by Hessian fly larvae. *Plant Physiology and Biochemistry* **48,** 54–61.

Saltzmann KD, Giovanni MP, Zheng C, Williams CE. 2008. Virulent Hessian fly larvae manipulate the free amino acid content of host wheat plants. *Journal of Chemical Ecology* **34,** 1401–1410.

Sardesai N, Subramanyam S, Nemacheck JA, Williams CE. 2005. Modulation of defense-response gene expression in wheat during Hessian fly larval feeding. *Journal of Plant Interactions* **1,** 39–50.

Schönherr J. 1982. Resistance of plant surfaces to water loss: transport properties of cutin, suberin and associated lipids. In: Lange OL, Nobel PS, Osmond CB, Ziegler H, eds. *Encyclopedia of plant physiology*, Vol. 12B.. Berlin: Springer, 153–179.

Schreiber L, Krimm U, Knoll D, Sayed M, Auling G, Kroppenstedt RM. 2005. Plant–microbe interactions: identification of epiphytic bacteria and their ability to alter leaf surface permeability. *New Phytologist* **166,** 589–594.

Shukle RH, Grover PB, Mocelin G. 1992. Responses of susceptible and resistant wheat associated with Hessian fly (Diptera: Cecidomyiidae) infestation. *Environmental Entomology* **21,** 845–853.

Singh MK. 2000. Rotational relaxation of neutral red in alkanes: effects of solvent size on probe rotation. *Photochemistry and Photobiology* **72,** 438–443.

Sosa O, Gallun RL. 1973. Purification of races B and C of the Hessian fly by genetic manipulation. *Annals of the Entomological Society of America* **66,** 1065–1070.

Subramanyam S, Smith DF, Clemens JC, Webb MA, Sardesai N, Williams CE. 2008. Functional characterization of HFR1, a high-mannose N-glycan-specific wheat lectin induced by Hessian fly larvae. *Plant Physiology* **147,** 1412–1426.

Yeats TH, Howe KJ, Matas AJ, Buda GJ, Thannhauser TW, Rose JKC. 2010. Mining the surface proteome of tomato (*Solanum lycopersicum*) fruit for proteins associated with cuticle biogenesis. *Journal of Experimental Botany* **61,** 3759–3771.